MEMO 4-30-59E

NASA

MEMORANDUM

EXPERIMENTAL INVESTIGATION OF GAS-SIDE PERFORMANCE

OF A COMPACT FINNED-TUBE HEAT EXCHANGER

By Louis Gedeon

Lewis Research Center
Cleveland, Ohio

NATIONAL AERONAUTICS AND
SPACE ADMINISTRATION

WASHINGTON
May 1959
Declassified July 11, 1961

NATIONAL AERONAUTICS AND SPACE ADMINISTRATION

MEMORANDUM 4-30-59E

EXPERIMENTAL INVESTIGATION OF GAS-SIDE PERFORMANCE OF A COMPACT FINNED-TUBE HEAT EXCHANGER

By Louis Gedeon

SUMMARY

Heat-transfer and pressure-drop data were obtained experimentally for the gas side of a liquid-metal to air, compact finned-tube heat exchanger. The heat exchanger was fabricated from 0.185-inch Inconel tubing in an inline array. The fins were made of 310 stainless-steel-clad copper with a total thickness of 0.010 inch, and the fin pitch was 15.3 fins per inch. The liquid used as the heating medium was sodium. The heat-exchanger inlet gas temperature was varied from 510° to 1260° R by burning JP fuel for airflow rates of 0.4 to 10.5 pounds per second corresponding to an approximate Reynolds number range of 300 to 9000. The sodium inlet temperature was held at 1400° R with the exception of a few runs taken at 1700° and 1960° R. The maximum ratio of surface temperature to air bulk temperature was 1.45.

Friction-factor data with heat transfer were best represented by a single line when the density and viscosity of Reynolds number were evaluated at the average film temperature. At the lower Reynolds numbers reported, the friction data with heat transfer plotted slightly above the friction data without heat transfer. The density of the friction factor was calculated at the average bulk temperature.

Heat-transfer results of this investigation were correlated by evaluating the physical properties of air (specific heat, viscosity, and thermal conductivity) at the film temperature.

INTRODUCTION

Liquid-metal to air heat exchangers are required for certain types of nuclear-powered aircraft. The heat picked up inside the reactor is transferred in the heat exchanger to the compressor discharge air before its entry into the turbine. Heat exchangers are also required for nuclear space vehicles using a secondary fluid to heat the propellant gas. As in the nuclear airplane, heat is picked up in the reactor by a fluid such as sodium in a closed loop and is transferred to a gas before being exhausted through a nozzle. A compact finned-tube heat exchanger using liquid sodium was fabricated and tested in a previous investigation at NASA Lewis Research Center (ref. 1). Because of weld failures, only pressure-drop data without sodium flow were obtained. The present report gives experimental air-side heat-transfer results for a modified version of this type heat exchanger.

The heat exchanger tested was fabricated of 0.185-inch Inconel tubing in an inline array. The center-to-center spacing of each tube in a bank, as well as the spacing of each bank, was 0.667 inch. The fins, formed from 0.010-inch-thick stainless-steel-clad copper plates, were continuous across each bank of twelve tubes and were three banks deep. The fin pitch was 15.3 fins per inch.

Tests on the air-side performance, using sodium as the heating fluid, were conducted in a 500-kilowatt facility at Lewis Research Center. The inlet air temperature was varied from approximately 510° to 1260° R by burning JP fuel for a sodium temperature of 1400° R with a maximum surface-temperature to air-bulk-temperature ratio of 1.43.

The data of this report did not coincide with known heat-transfer and friction-factor correlations, nor with data of other extended-surface heat exchangers of similar design. Therefore, heat-transfer and pressure-drop data of only the heat exchanger tested are presented.

SYMBOLS

All symbols are of consistent units and refer to the air side of the heat exchanger unless otherwise noted.

A	minimum flow area
c_p	specific heat at constant pressure
D	hydraulic diameter, 4 AL/S
F	fin heat-transfer surface area
f	friction factor
G	mass flow per unit cross-sectional area, w/A
g	gravitational constant

h average heat-transfer coefficient

K average thermal conductivity of fin

k thermal conductivity

L heat-transfer length of heat exchanger

l fin height

Nu Nusselt number

Pr Prandtl number

p absolute static pressure

Δp static-pressure difference

R gas constant for air

Re Reynolds number

S total heat-transfer area

T temperature, $^{\circ}R$

T_b average air bulk temperature defined as $(T_1 + T_2)/2$, $^{\circ}R$

T_f average film temperature defined as $T_s - 0.5\,\Delta T_m$, $^{\circ}R$

ΔT_m log mean temperature difference, $\dfrac{(T_1 - T_4)-(T_2 - T_3)}{\ln \dfrac{T_1 - T_4}{T_2 - T_3}}$

T_s average surface temperature defined as average sodium temperature, $^{\circ}R$

V velocity

w airflow rate

δ fin thickness

η fin efficiency

η_o fin effectiveness

μ absolute viscosity

ρ density

Subscripts:

av average

b bulk (when applied to properties, indicates evaluation at temperature T_b)

Cu copper

f film (when applied to properties, indicates evaluation at temperature T_f)

fr friction

Na sodium

s surface

ss 310 stainless steel

1,2 air stations upstream and downstream of heat exchanger

3,4 sodium stations entering and leaving heat exchanger

APPARATUS

A schematic diagram of the test facility used to obtain average heat-transfer and pressure-drop data for the finned-tube heat exchanger is shown in figure 1. A sodium loop and an air tunnel make up the test apparatus. Sodium is circulated by a centrifugal pump that is driven by a variable-speed motor. The components making up the sodium loop are the circulating pump, an electric resistance heater, the tube side of the heat exchanger, a volume-measuring tank, and the sump tank. The air side of the facility consists of a flow-regulating valve, an orifice, a fuel burner, the finned side of the heat exchanger, and a downstream pressure-regulating valve.

A brief description of the apparatus is given herein; for more detailed information see reference 1.

Air Tunnel

Air is supplied through a 6-inch line at a pressure of 120 pounds per square inch. Airflow rates are controlled by the upstream butterfly valve and are measured by a standard 6-inch sharp-edge flange-type orifice assembly (see fig. 1). An altered J-35 burner-can assembly is used to preheat the air to a desired temperature. To get the maximum air temperature, a fuel-air ratio of less than 0.015 was required. For such a fuel-air ratio, the gas properties of the mixture are essentially those of air. This mixture is referred to as air hereinafter. Baffles in a 30-inch-diameter section located downstream of the burner mix the air thoroughly to give a uniform temperature distribution. A 16-mesh stainless-steel screen mounted at the entrance of the heat-exchanger tunnel reduces large-scale turbulence that may exist and also serves as a trap for particles formed during burning of the fuel that could lodge between the fins. The heat-exchanger pressure level is set by the pressure drop taken across the downstream butterfly valve.

Sodium Loop

Sodium is stored in the sump tank and at all times has a protective atmosphere of argon. The centrifugal pump housed in the sump tank has a capacity of 50 gallons per minute and is driven by a 30-hp variable-speed motor. Sodium flow rates are measured by noting the time required to fill a known volume within the volume-measuring tank. A vent line connecting the volume measuring tank and the sump tank allows argon to flow from one tank to the other while a flow measurement is being made. The temperature of the sodium entering the heat exchanger is set and maintained by adjusting the power to the electric resistance heater. The capacity of the heater is 500 kilowatts at a maximum of 25 volts.

All components and piping of the sodium loop are fabricated from 300-series stainless steel, with the exception of the heat exchanger and electric resistance heater, which are formed from Inconel and Inconel X tubing, respectively. Connections between the pipe and components are made with stainless-steel O-ring-type flanges.

Heat Exchanger

The heat exchanger is a fin-tube type in a two-pass cross-flow arrangement. Each fin is continuous across each bank of twelve tubes, is three banks deep, and is furnace-brazed to the tubes. A photograph and a drawing of the heat exchanger are shown in figures 2(a) and (b). The basic dimensions and materials of the heat exchanger are:

Over-all size, in.	16 by 8 by 8
Tube size, in.	0.185 O.D., 0.025 wall
Number of tubes	144 (12 tubes/bank)

Tube material	Inconel
Tube spacing (transverse and longitudinal), in.	0.667
Tube arrangement	inline
Fin thickness, δ, in.	0.010
Fin material (clad)	0.005-in. copper with 0.0025-in. stainless-steel cladding
Number of fins per inch	15.3
Fin heat-transfer area, F, sq ft	198
Total heat-transfer area, S, sq ft	204
Minimum airflow area, A, sq ft	0.557
Air-side equivalent diameter, D, ft	0.00730

The heat exchanger extends through the bottom of the rectangular stainless-steel tunnel and is supported by the sodium lines that are welded to the pressure shell (see fig. 2(c)). The heat exchanger is not fastened to the tunnel. This assembly leaves a gap between the heat exchanger and the bottom plates of the tunnel where air may enter or escape to the shell volume. To minimize heat loss and to further minimize air bypassing the heat exchanger, the shell volume is packed with glass wool.

The tunnel is supported so that its expansion is away from the heat exchanger. This expansion is taken up by a bellows at the downstream end and a loose sliding fit into the forward air tunnel.

Instrumentation

Instrumentation for air heat-transfer and pressure-drop data is located at stations 7 inches before and after the heat exchanger. The upstream station has nine total-temperature thermocouples and nine total-pressure tubes positioned in the center of equal rectangular areas. The downstream side is divided into twelve equal rectangular areas. Both stations have four static-pressure taps located on the walls of the tunnel, in the same plane as the total-pressure tubes.

Sodium temperatures are measured by three thermocouples located before the heat exchanger and three couples located after the heat exchanger. Stainless-steel tubing incases each of the thermocouples and projects into the sodium stream so that at least twenty thermocouple tube diameters run parallel to the direction of sodium flow. The relative positions are indicated as stations 3 and 4 in figure 2(c). All thermocouples are made of 24-gage Chromel-Alumel wire.

All pressures are indicated on banks of manometers that are photographed to simplify the recording of data and provide a permanent record. Temperatures are read on a self-balancing recording-type potentiometer.

No attempt was made to instrument the fins or tubes of the heat exchanger. The compactness of the heat exchanger makes it virtually impossible to attach thermocouples that would not interfere with the normal airflow pattern through the heat exchanger.

TEST PROCEDURE

Pressure-drop data were taken with and without heat transfer. For isothermal conditions, the airflow and fuel-flow rates were set to give a desired air temperature. After equilibrium was reached, airflow rate, pressure, and temperature were recorded. Another run was set by changing the air and fuel-flow rates while the air temperature was kept constant. The procedure was repeated for temperature levels of 510°, 860°, 1060°, and 1260° R with airflow rates of 0.4 to 10 pounds per second. These limits were determined by the capacity of the system.

The following procedure was used to obtain experimental data with heat transfer. Before starting sodium flow, the entire sodium loop was preheated to about 760° R with the exception of the sump tank, which was heated to 1000° R. The higher sump temperature was used in order to allow flow past cold areas when sodium flow was first started.

Air- and fuel-flow rates were set for the desired heat-exchanger inlet air temperature. The sodium pump was started, and the flow was adjusted to approximately 3 pounds per second. Power to the electric resistance heater was adjusted to elevate the sodium temperature from 1000° to 1400° R, and it was again adjusted to balance the heat given up in the heat exchanger. The airflow rate and heat-exchanger inlet air temperature were varied in the same manner as for runs without heat transfer.

The ring-joint flanges used to connect the individual components of the sodium loop failed to keep a leak-tight system for a sodium temperature of 1960° R. However, a few runs were made with sodium inlet temperatures of 1700° and 1960° R before the flanges failed. The data taken at these higher sodium temperatures coincided with the results obtained for a sodium temperature of 1400° R; and, therefore, the data taken after the flange failure were restricted to a sodium temperature of 1400° R. The data reported were taken before and after the failure.

From the indication of the data taken, a period of approximately 4 hours of sodium flow was required before all the argon gas was forced from the heat exchanger. The initial calculated Nusselt numbers for each startup were low, but after a period of time the data increased to values presented in this report.

METHOD OF CALCULATION

The diagram shown in figure 2(c) represents the heat exchanger, its surroundings, and the stations used in the calculation of the average friction factor and heat-transfer coefficient.

Total temperature, total pressure, and static pressure were measured at stations 1 and 2. Sodium temperature was measured at stations 3 and 4.

Friction Factor

Average friction factors for isothermal and heat-transfer runs were calculated from the friction pressure drop by use of the conventional relation,

$$f = \Delta p_{fr} 2g\rho_{av} \Big/ 4G^2(L/D)$$

The hydraulic diameter D is defined as

$$D = 4(AL/S)$$

The length L is 8 inches, the distance from leading edge of the front fin to the trailing edge of the back fin.

Substituting the equivalent for D in the friction-factor equation gives the following relation:

$$f = \Delta p_{fr} 2g\rho_{av} \Big/ G^2(S/A)$$

The friction pressure drop Δp_{fr} was obtained by subtracting the momentum pressure drop from the over-all static-pressure drop. The inlet and exit losses are included as part of the friction pressure drop:

$$\Delta p_{fr} = \Delta p_{1-2} - \frac{G^2}{g}\left(\frac{1}{\rho_2} - \frac{1}{\rho_1}\right)$$

The average density ρ_{av} was calculated at the average pressure and temperature, as determined from stations 1 and 2:

$$\rho_{av} = \frac{p_1 + p_2}{R(T_1 + T_2)}$$

The Mach number ahead of and after the heat exchanger was less than 0.1, and therefore the total temperature measured was assumed to be equal to static temperature.

Inlet and outlet air temperature and pressures were evaluated as the arithmetic average of the individual probes. The instrumentation ahead of the heat exchanger showed no variation in temperature and pressure across the flow area. The pressure probes downstream of the heat exchanger also indicated no variations, while the thermocouples showed a random variation for a few runs of large air-temperature rise with a maximum difference of about 20°.

Heat-Transfer Coefficient

Average heat-transfer coefficients for the air side of the heat exchanger were calculated from the following equation:

$$h = wc_p(T_2 - T_1)/S\ \Delta T_m \eta_o$$

The film temperature drop on the sodium side and the temperature drop through the tube wall are negligible compared with the temperature drop through the air film. It was therefore assumed that all the temperature drop occurs on the air side and that the average primary surface temperature T_s is equal to the average of the sodium temperatures entering and leaving the heat exchanger.

Fin effectiveness η_o is a function of fin efficiency and both the fin and total heat-transfer areas, as given by the following equation obtained from reference 2:

$$\eta_o = 1 - \frac{F}{S}(1 - \eta)$$

No data are available to determine the fin efficiency η of this heat exchanger directly. Information is available, however, on disc-type fins. In order to use this information to determine the fin efficiency of the continuous-type fins of this heat exchanger, an equivalent disc fin having the same surface area per tube was calculated. This resulted in an equivalent disc fin with a fin diameter equal to four times the tube diameter. The curve of fin efficiency used in this report is shown in figure 3. This curve is for disc-type fins and was reproduced from reference 2.

The physical properties of air, specific heat, viscosity, and thermal conductivity were obtained from reference 3. The thermal conductivity of the fin (50 percent copper and 50 percent 310 stainless-steel cladding) was evaluated as the average of the thermal conductivities of the two metals. The values were obtained from reference 4 and were calculated from the following equations:

Copper:

$$K_{Cu} = 236.2 - 0.02\ T$$

310 Stainless steel:

$$K_{ss} = 5.387 + 0.00589\ T$$

where T_s is given in $^{\circ}R$ and K is given in Btu/(hr)(sq ft)($^{\circ}$F)/ft.

The primary surface temperature was used to evaluate the thermal conductivity of the fins. The coefficients of temperature of the preceding equations are small, and using a temperature more identical with a true average fin temperature will have only a small percentage effect on the value of the fin thermal conductivity. The error is further decreased by the fact that the fin efficiency is a function of the square root of the fin thermal conductivity (see fig. 3).

RESULTS AND DISCUSSION

The basic data obtained in this investigation with and without heat transfer are shown in tables I and II. The Reynolds number range covered for isothermal data was from 300 to 9000, and the range for heat-transfer data was 300 to 6000. Except for a few runs the average sodium temperature was held at approximately 1400° R.

A comparison of the calculated heat transferred to the air and the heat lost by the sodium gave heat-balance results that were within 10 percent, the major part of the data being within 5 percent.

Friction Factor

The experimental friction-factor data with no heat addition are shown in figure 4; friction factor f is plotted against Reynolds number GD/μ_b. The data represent four temperature levels with inlet air pressures varying from zero to about 60 pounds per square inch gage. The solid line is the best line through the data and is used for comparison with heat-transfer friction data.

Figure 5(a) shows the friction-factor data with heat addition, where the friction f is plotted against Reynolds number GD/μ_b. The data were divided into four groups of primary surface-temperature to air-bulk-temperature ratios. The dashed lines connect the data of each of these T_s/T_b groups. The solid line represents the isothermal data of figure 4. There is a marked separation of data in the transition region showing a trend with the surface-temperature to air-bulk-temperature ratio.

Because of the limits of the system, no large ratios of surface to air-bulk temperatures are presented for the higher airflow rates.

To eliminate the trend with temperature ratio shown in figure 5(a), the friction-factor data were plotted against a film Reynolds number $\rho_f VD/\mu_f$. The reevaluated data are shown in figure 5(b). The density in the friction factor was not altered. The data of the lower Reynolds numbers fall slightly above the friction-factor data without sodium flow. Evaluating the Reynolds number at a temperature greater than the film temperature would increase the scatter of the data. If the density of the friction factor were calculated at the same temperature as that used to determine Reynolds number, the data would show a separation similar to that of figure 5(a).

The data without heat transfer (fig. 4) were taken after heat-transfer results were obtained. Thus, any permanent change in the alinement of the heat exchanger, resulting from use in heat-transfer tests, was present throughout the entire series of tests. Enough warpage may occur in the heat exchanger with sodium flow, because of the sodium temperature drop, to misaline the fins and increase the pressure drop.

Heat-Transfer Coefficient

The majority of heat-transfer data was obtained for an inlet sodium temperature of 1400° R. A few runs were taken with sodium inlet temperatures of 1700° and 1960° R.

Heat-transfer results are shown in figure 6(a), where the film Nusselt number divided by the film Prandtl number raised to the 0.4 power ($Nu_f/Pr_f^{0.4}$) is plotted against the film Reynolds number ($\rho_f VD/\mu_f$). There seems to be a separation of data for the four surface-temperature to air-bulk-temperature ratios indicated. Evaluating the data on a surface-temperature basis would increase the scatter.

A better arrangement of data, to give less scatter, was obtained when the density of the Reynolds number term was based on a bulk temperature. Figure 6(b) is a replot of figure 6(a) with the exception that the density was evaluated at the bulk temperature. The solid line of figure 6 represents the best straight line through the data.

It should be pointed out that the majority of the data presented in this report was obtained in what may be classified as the transition region. These results may not apply to the higher Reynolds number region of turbulent flow.

The exact values of fin efficiency and fin thermal conductivity could not be determined. However, the fin efficiency used and the value of fin thermal conductivity as calculated in this report should be close to the exact values. Any change made to refine the data of these two properties would only slightly alter the magnitude of each data point and thus would not affect the over-all results of this report.

Although it is not very satisfying to have different correlations for heat-transfer and friction-factor data (the density of Reynolds number was based on different temperatures), a common correlation could not be achieved.

Correlation of Extended-Surface Heat Exchangers

A correlation obtained from heat exchangers using spiral fins and based on an equivalent diameter defined in terms of tube spacing, tube diameter, and fin diameter is given in reference 5. A friction-factor correlation based on an equivalent volumetric diameter is presented in reference 6. The data of this investigation were lower than the results given in references 5 and 6. Heat-transfer and pressure-drop data of many different compact heat exchangers may be found in reference 7. Because the geometry of the heat exchangers in reference 7 did not coincide with that used herein, the fact that the present data did not agree with the results of reference 7 is not entirely surprising. An extensive analysis of extended-surface data would be required to correlate the results of the many configurations possible.

SUMMARY OF RESULTS

Heat-transfer and pressure-drop data were obtained experimentally for the gas side of a liquid-metal to air, finned-tube heat exchanger. The heat exchanger was constructed from 0.135-inch tubing in an inline array with 0.667-inch center-to-center spacing. The fins were of the continuous type, stainless-steel-clad copper, 0.010-inch thick and furnace-brazed to the tubes. The fin pitch was 15.3 fins per inch.

Inlet air temperature was varied from 510° to 1260° R by burning JP fuel for a range of Reynolds numbers of 300 to 9000 corresponding to airflow rates of 0.4 to 10.5 pounds per second. Sodium inlet temperature was held at 1400° R for most of the runs, and a few check points were taken for inlet temperatures of 1700° and 1960° R. The following results are indicated:

1. Friction factors with heat transfer were best represented by a single line when the density and viscosity of Reynolds number were

evaluated at the average film temperature. The data of the lower Reynolds number region fell slightly above the results obtained without heat transfer. The density of friction factor was evaluated at the bulk temperature.

2. Heat-transfer results were correlated by evaluating the physical properties of air (specific heat, viscosity, and thermal conductivity) at the film temperature.

Lewis Research Center
National Aeronautics and Space Administration
Cleveland, Ohio, February 2, 1959

REFERENCES

1. Gedeon, Louis, Conant, Charles W., and Kaufman, Samuel J.: Experimental Investigation of Air-Side Performance of Liquid-Metal to Air Heat Exchangers. NACA RM E55L05, 1956.

2. Gardner, Karl A.: Efficiency of Extended Surface. Trans. ASME, vol. 67, no. 8, Nov. 1945, pp. 621-631.

3. Hilsenrath, Joseph, et al.: Tables of Thermal Properties of Gases. Cir. 564, NBS, Nov. 1, 1955.

4. Perry, John H., ed.: Chemical Engineers' Handbook. Third ed., McGraw-Hill Book Co., Inc., 1950, p. 456.

5. Jameson, B. L.: Tube Spacing in Finned-Tube Banks. Trans. ASME, vol. 67, no. 8, Nov. 1945, pp. 633-642.

6. Gunther, A. Y., and Shaw, W. A.: A General Correlation of Friction Factors for Various Types of Surface in Crossflow. Trans. ASME, vol. 67, no. 8, Nov. 1945, pp. 643-660.

7. Kays, W. M., and London, A. L.: Compact Heat Exchangers. National Press, 1955.

TABLE I. - BASIC ISOTHERMAL PRESSURE-DROP DATA[a]

T_b, °R	p_1, lb/sq ft	w, lb/sec	Δp_{1-2}, in. water	f	Re	T_b, °R	p_1, lb/sq ft	w, lb/sec	Δp_{1-2}, in. water	f	Re
531	2109	0.42	0.30	0.0355	455	865	8337	8.50	20.65	0.0146	6407
525	2113	.60	.46	.0272	651	1049	2126	.61	1.27	.0374	402
522	2109	.92	.87	.0222	1001	1050	2117	.70	1.52	.0338	461
514	2140	1.50	1.86	.0184	1649	1060	2127	1.04	2.59	.0258	682
521	2147	2.02	3.26	.0176	2192	1070	2150	1.23	3.33	.0237	802
535	2212	3.03	7.15	.0171	3225	1069	2159	1.69	5.38	.0203	1102
528	2275	4.27	12.80	.0159	4593	1075	2180	1.82	6.00	.0197	1180
528	6346	7.09	11.40	.0145	7626	1063	2187	2.05	7.29	.0189	1345
528	7630	8.87	14.35	.0141	9541	1060	2233	2.59	10.85	.0179	1701
860	2131	.56	.85	.0366	420	1055	4161	4.20	12.60	.0160	2769
885	2123	.88	1.64	.0270	655	1070	6636	6.35	18.55	.0152	4141
850	2139	1.25	2.56	.0222	950	1055	9346	9.56	27.05	.0144	6298
845	2136	1.39	2.90	.0204	1060	1260	2128	.50	1.36	.0492	294
870	2166	1.99	5.70	.0190	1497	1268	2121	.51	1.33	.0464	298
855	3114	3.41	10.55	.0176	2586	1255	2132	.85	2.54	.0322	500
860	3913	4.65	15.00	.0168	3514	1258	2161	1.36	4.77	.0238	798
850	6307	6.42	15.85	.0152	4893	1241	2173	1.65	6.20	.0212	980

[a]Data were not taken in order shown.

TABLE II. - BASIC HEAT-TRANSFER DATA[a]

T_s/T_b	T_b, ^oR	ΔT_{air}, ^oR	T_s, ^oR	ΔT_{Na}, ^oR	p_1, lb/sq ft	Δp_{1-2}, in. water	w, lb/sec	f	$\frac{\rho_f VD}{\mu_f}$	$\left(\frac{Nu}{Pr^{0.4}}\right)_f$	η_o
1.40	986	825	1377	126	2124	1.43	0.47	0.0707	219	2.18	0.93
1.44	978	855	1410	99	2122	1.50	.52	.0605	236	2.14	.93
1.43	963	855	1380	140	2136	2.45	.80	.0425	368	3.41	.90
1.43	942	823	1344	160	2139	2.95	.96	.0360	453	4.00	.89
1.42	913	776	1299	188	2143	3.47	1.15	.0297	567	4.58	.88
1.42	923	746	1307	203	2159	4.30	1.34	.0271	665	4.89	.87
1.45	888	725	1289	239	2164	5.25	1.61	.0232	813	5.21	.87
1.22	1547	694	1891	150	2152	3.90	.75	.0493	316	2.37	.90
1.23	1132	577	1397	113	2135	2.32	.71	.0452	349	3.26	.90
1.23	1144	557	1406	161	2147	3.60	.99	.0349	499	3.82	.89
1.20	1522	639	1833	228	2205	7.55	1.35	.0301	591	4.11	.86
1.21	1492	594	1798	252	2244	9.70	1.67	.0262	744	4.61	.85
1.24	1107	503	1368	151	10483	1.35	1.59	.0243	823	5.49	.85
1.24	1085	472	1341	248	2210	8.50	1.95	.0225	10379	5.84	.85
1.24	1094	468	1361	198	13262	1.67	2.18	.0313	11410	6.39	.84
1.14	1249	349	1425	50	2134	2.20	.64	.0480	327	2.49	.91
1.14	1446	429	1652	95	3993	1.85	.81	.0411	378	2.91	.89
1.16	1405	486	1636	108	2146	3.54	.82	.0418	383	3.02	.89
1.14	1242	391	1418	94	2141	3.08	.83	.0397	427	3.73	.88
1.14	1238	354	1415	82	7884	1.10	1.02	.0352	527	3.68	.87
1.14	1235	378	1411	122	2157	4.35	1.13	.0308	586	4.31	.87
1.16	1400	468	1624	142	2189	5.90	1.25	.0303	592	4.31	.86
1.18	1373	470	1613	180	2215	8.15	1.62	.0254	774	4.87	.85
1.14	1225	347	1395	149	2180	6.50	1.52	.0257	802	5.05	.86
1.15	1212	331	1392	114	1040	1.47	1.61	.0250	852	4.95	.86

[a]Data were not taken in order shown.

TABLE II. - CONCLUDED. BASIC HEAT-TRANSFER DATA[a]

T_s/T_b	T_b, ^oR	ΔT_{air}, ^oR	T_s, ^oR	ΔT_{Na}, ^oR	p_1, lb/sq ft	Δp_{1-2}, in. water	w, lb/sec	f	$\frac{\rho_f VD}{\mu_f}$	$\left(\frac{Nu}{Pr^{0.4}}\right)_f$	η_o
1.17	1363	415	1592	204	2283	11.45	2.07	0.0225	1008	5.55	0.84
1.13	1215	291	1368	157	2215	8.72	1.91	.0223	1031	5.75	.85
1.14	1212	300	1385	142	13537	1.78	2.21	.0209	1180	6.10	.84
1.13	1184	255	1338	144	2279	13.20	2.60	.0189	1429	6.87	.83
1.13	1200	273	1357	170	14227	2.38	2.70	.0200	1469	7.46	.82
1.17	1112	305	1304	233	14459	3.40	3.43	.0191	1905	8.95	.80
1.14	1175	215	1342	205	4009	17.08	4.25	.0164	2335	8.64	.80
1.19	1098	292	1304	211	6081	11.40	4.32	.0171	2389	10.28	.78
1.13	1151	209	1304	197	4132	17.90	4.24	.0167	2480	9.91	.78
1.14	1128	170	1284	241	5610	25.30	6.42	.0155	3625	12.32	.75
1.13	1150	167	1303	241	10424	15.85	6.85	.0158	3834	13.25	.74
1.15	1059	173	1215	193	10339	15.05	6.92	.0158	4039	13.93	.74
1.15	1107	132	1274	262	8532	41.25	10.54	.0146	5938	16.26	.70
1.08	1349	210	1456	47	2152	3.90	.98	.0337	512	3.39	.89
1.06	1354	168	1441	47	2167	5.43	1.29	.0273	682	4.21	.87
1.07	1345	173	1439	58	10222	1.50	1.51	.0263	800	4.54	.86
1.07	1335	167	1429	72	2240	10.35	2.03	.0218	1082	5.67	.84
1.08	1238	129	1342	152	5608	19.55	5.31	.0163	2950	10.68	.77
1.07	1234	76	1317	135	9009	25.30	8.08	.0148	4549	13.49	.73
1.05	1315	50	1318	105	8924	46.00	10.54	.0147	5773	14.74	.70

[a]Data were not taken in order shown.

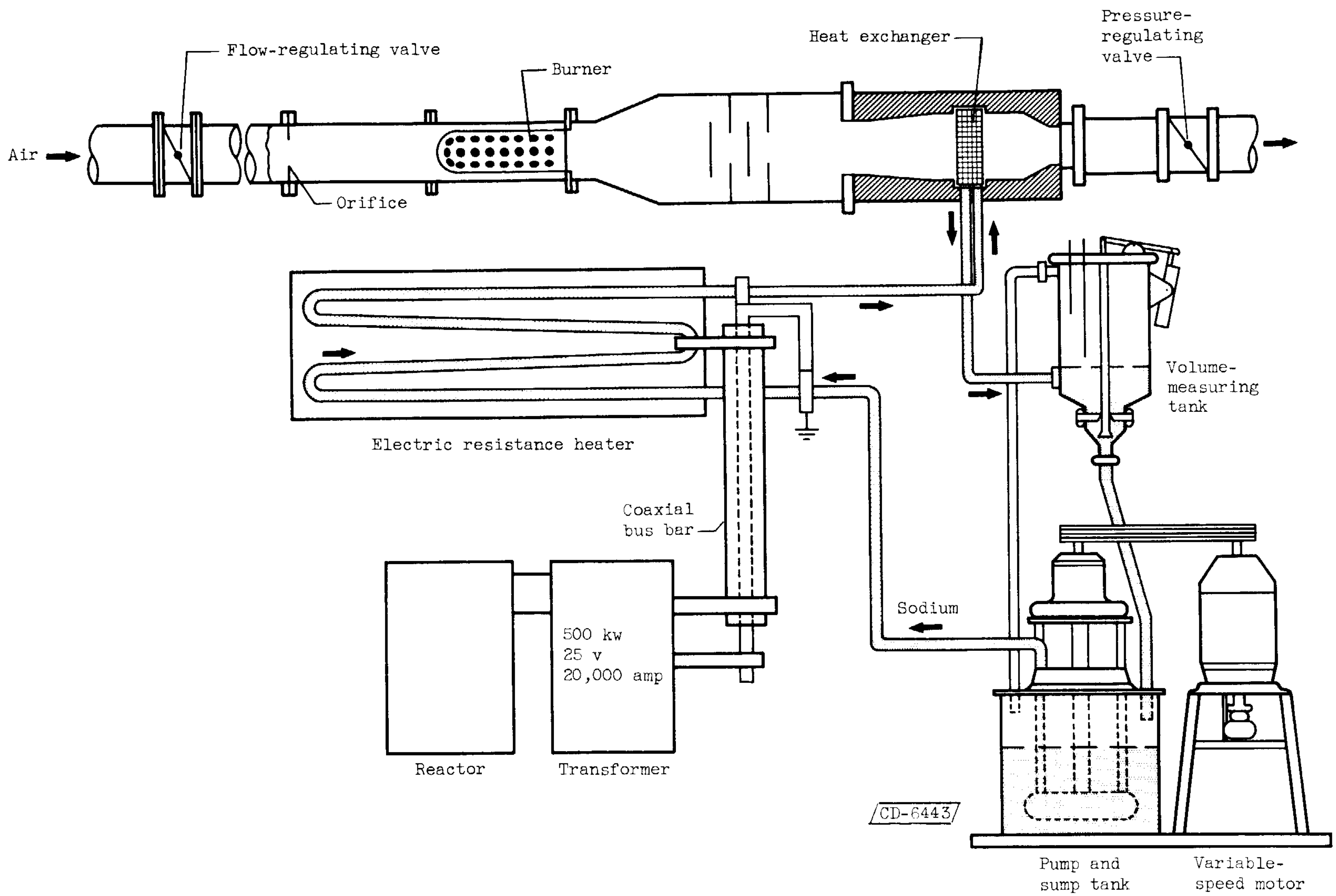

Figure 1. - Liquid-metal, 500-kilowatt heat-exchanger test facility.

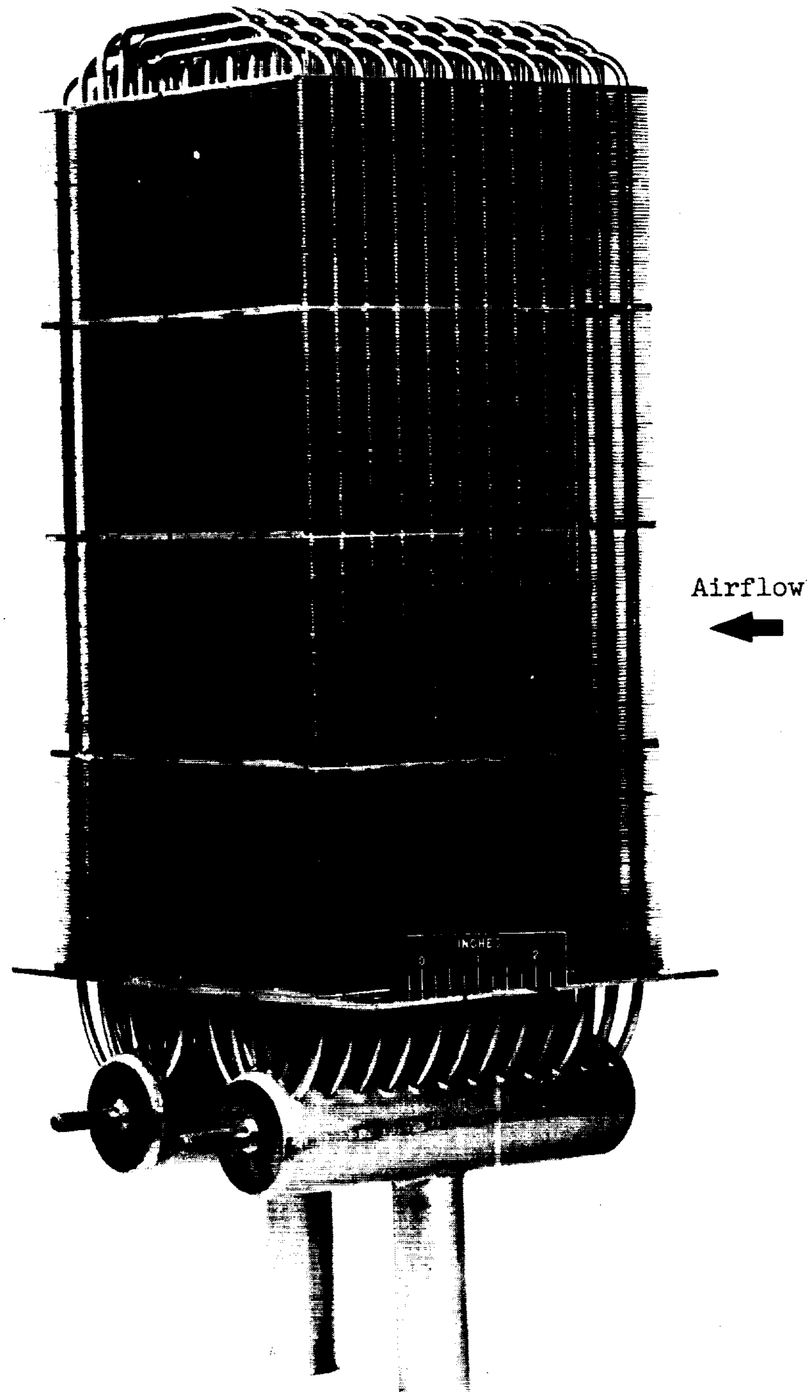

C-43140

(a) Photograph.

Figure 2. - Heat exchanger.

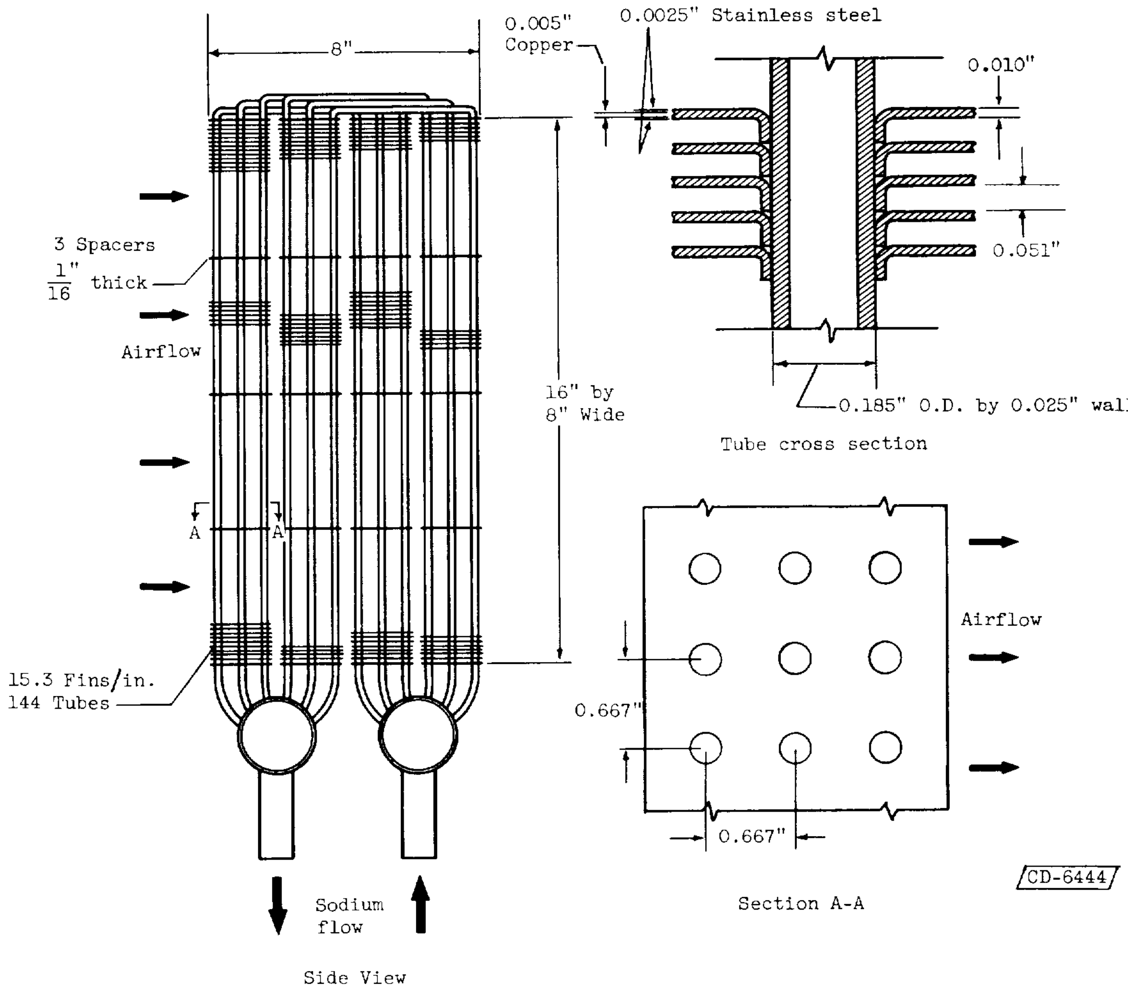

(b) Construction details of fins and tubes.

Figure 2. - Continued. Heat exchanger.

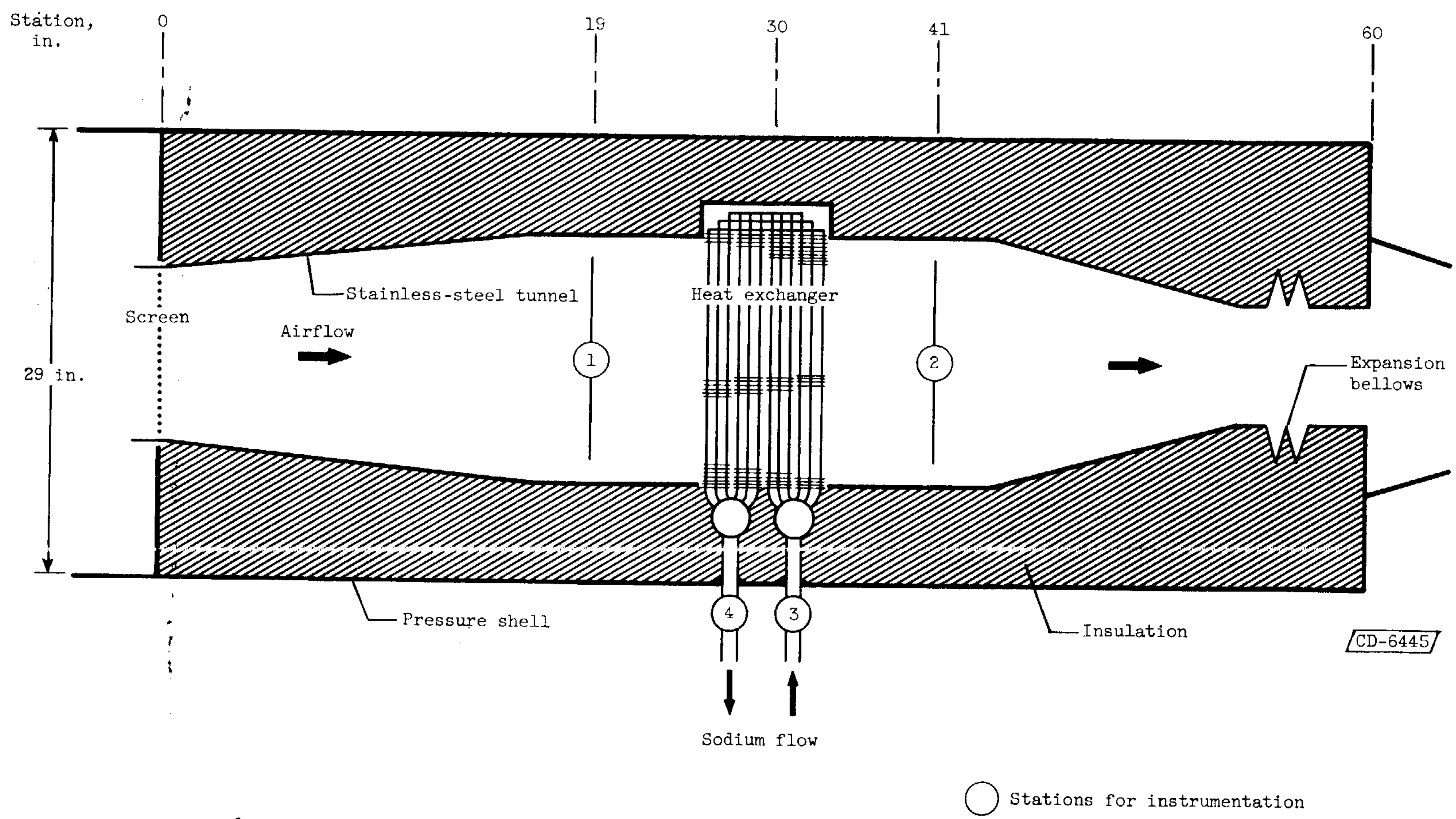

(c) Heat exchanger and surrounding area.

Figure 2. - Concluded. Heat exchanger.

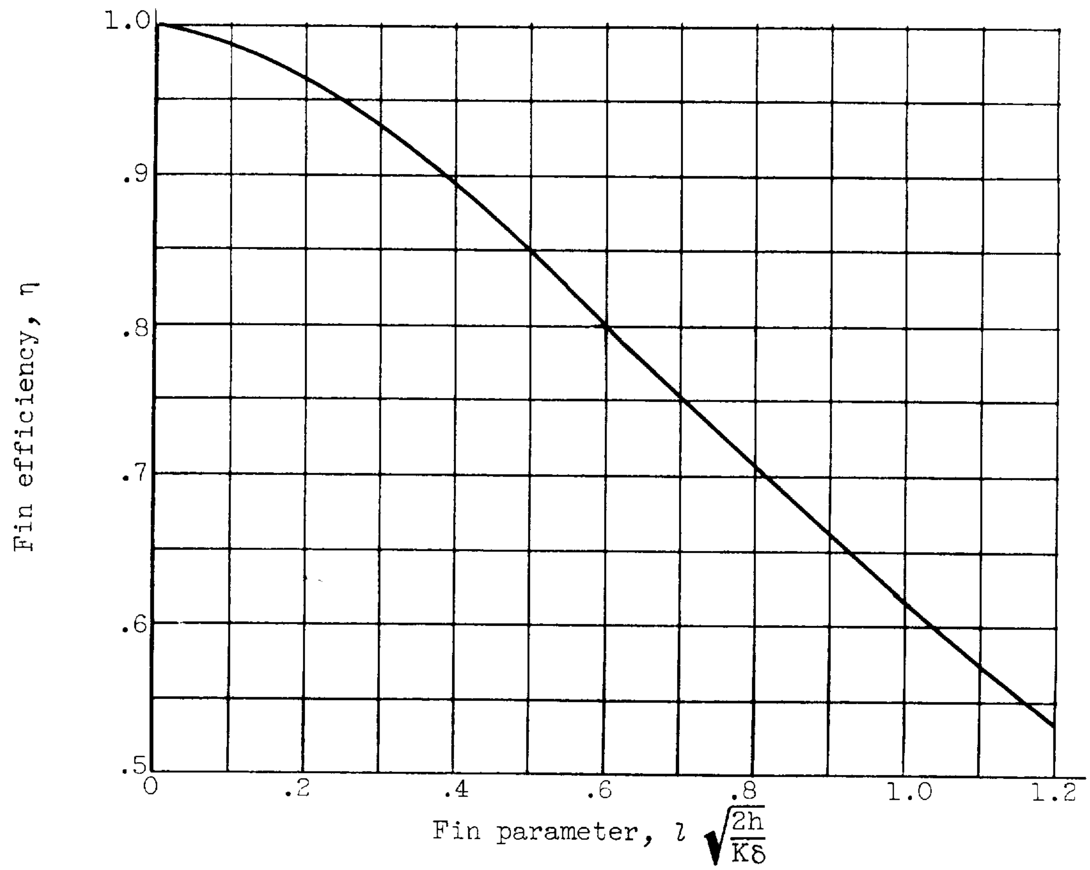

Figure 3. - Variation of fin efficiency for a fin-height to tube-radius ratio of 4 (data from ref. 2).

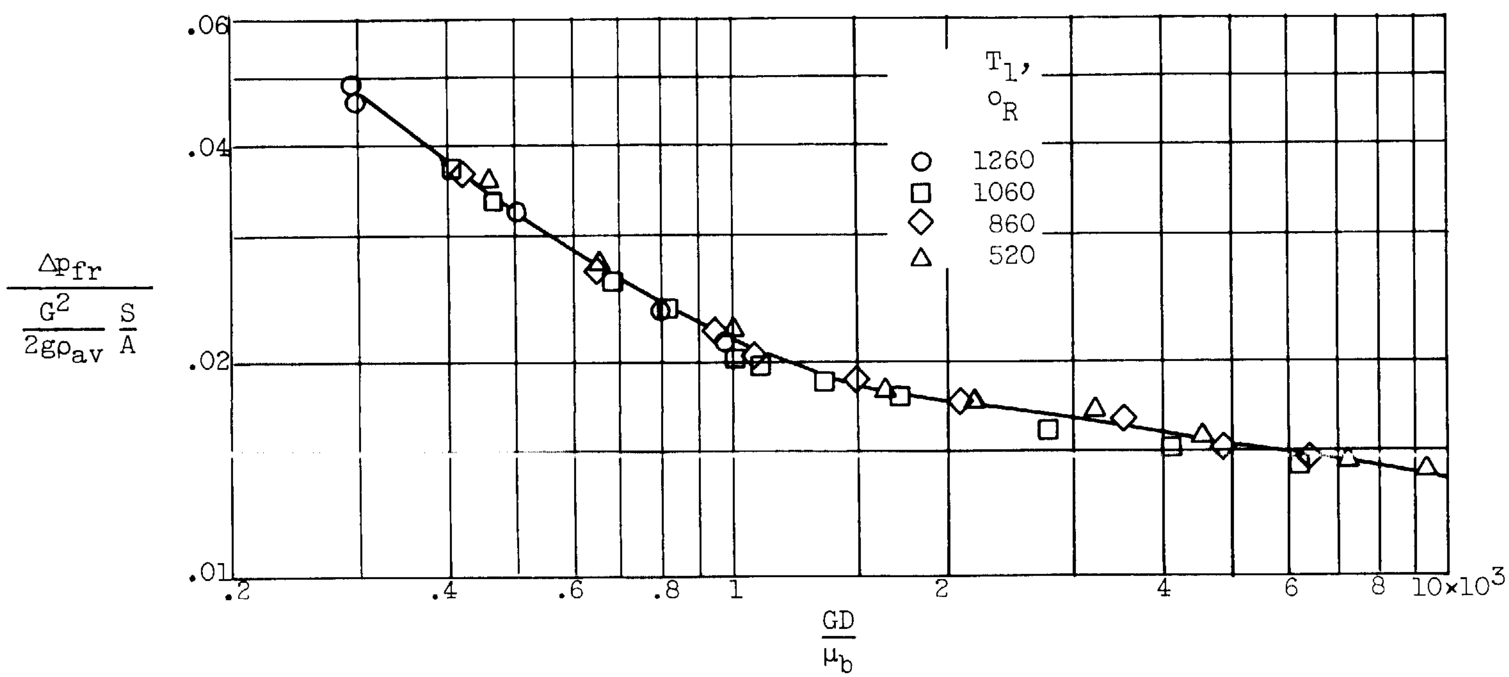

Figure 4. - Friction-factor data without heat transfer.

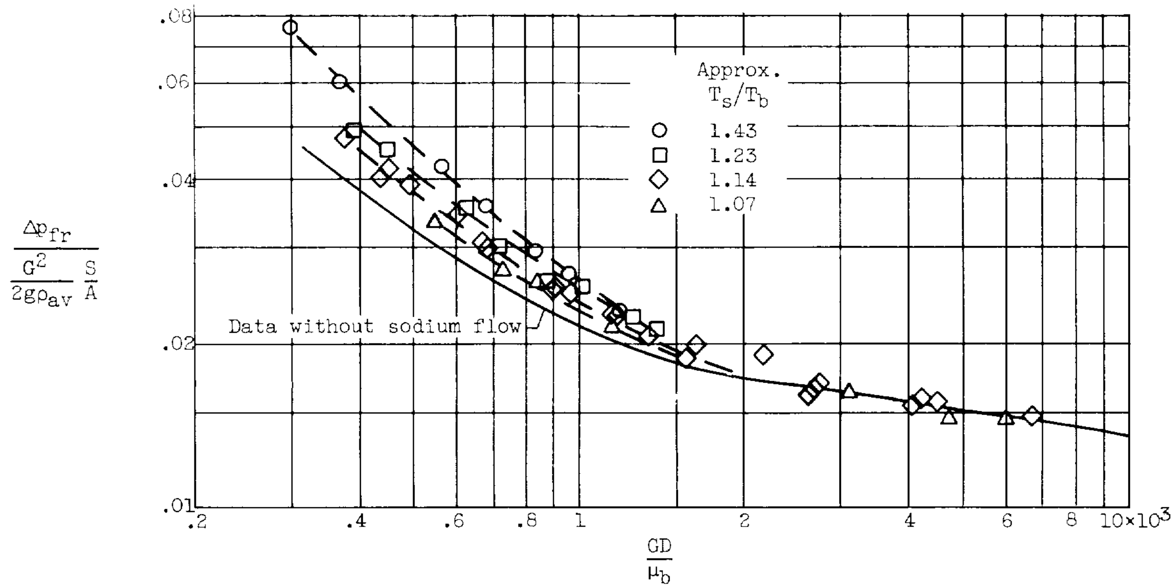

(a) Physical properties of air evaluated at bulk temperature, T_b.

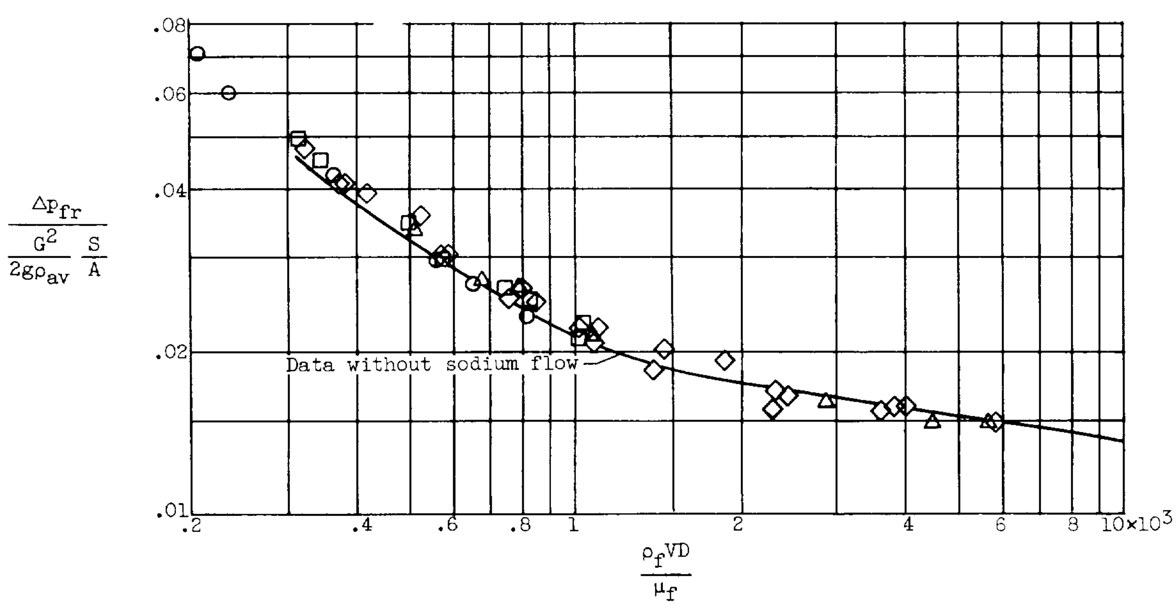

(b) Physical properties of air in Reynolds number (ρ and μ) evaluated at average film temperature, T_f.

Figure 5. - Friction-factor data with heat addition.

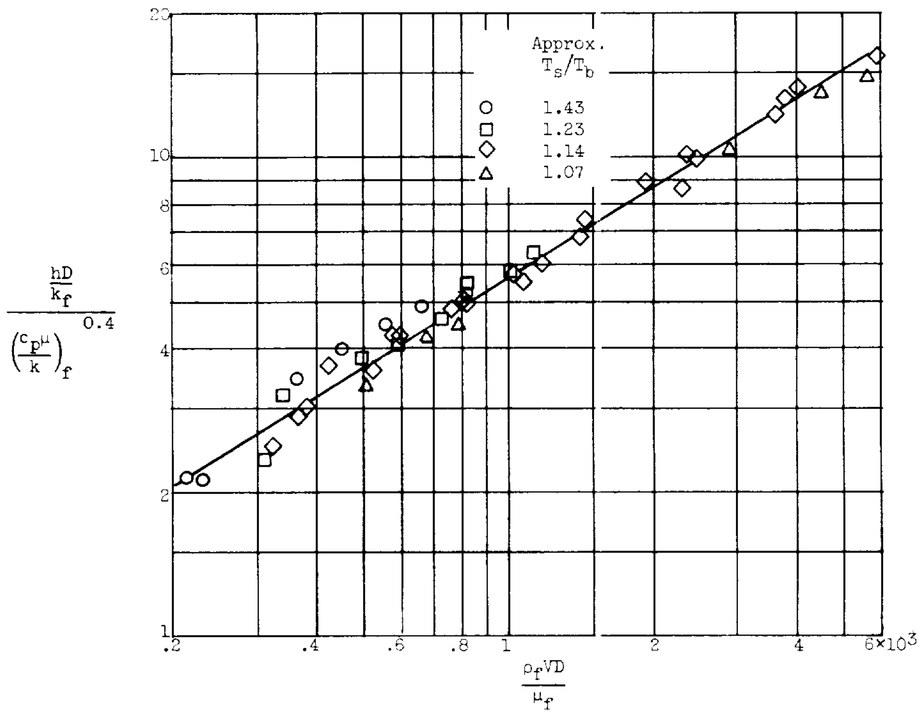

(a) All physical properties of air evaluated at film temperature, T_f.

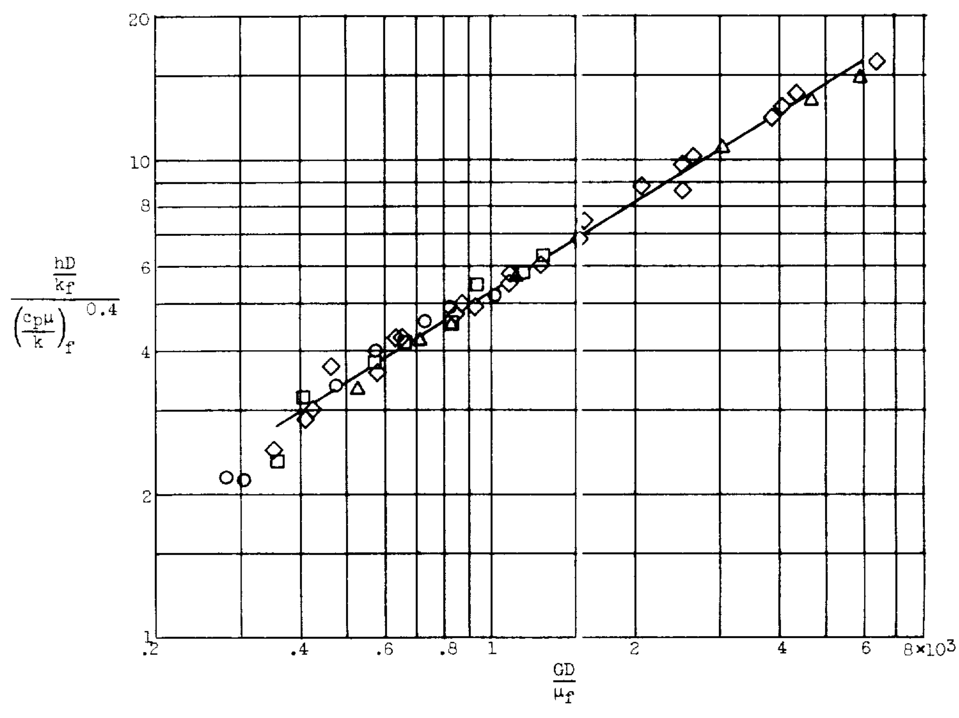

(b) Physical properties c_p, μ, and k evaluated at film temperature, T_f; density in Reynolds number based on bulk temperature, T_b.

Figure 6. - Heat-transfer data.